Mathematical Modelling of Weld Phenomena 6, eds H. Cerjak and H. K. D. H. Bhadeshia, published by Maney, London, 2002. pp. 231-242

Secondary effects in neural network analysis of the mechanical properties of welding alloys for HSLA shipbuilding steels

E. A. Metzbower
U. S. Naval Research laboratory

J. J. DeLoach
U. S. Navy Surface Warfare Center

Sree Harsha Lalam and H. K. D. H. Bhadeshia
University of Cambridge

Abstract

In previous work, we created neural network models for estimating the mechanical properties and toughness of alloys that are designed for the welding of high-strength low-alloy steels of the type intended for the construction of ships. The yield and ultimate strengths, the elongation and reduction-in-area, the Charpy toughness and dynamic tear properties were usefully modelled as a function of the chemical composition and the cooling rate. Ductility and toughness are complex properties; the purpose of the work presented here was to see if they could be modelled better by including the strength as an input.

Introduction

In previous work [1,2], the strength, ductility and fracture toughness of a series of experimental welding alloys were modelled using a neural network method [3-7] within a Bayesian framework. The models were based on a set of experimental data originating from a research programme with the aim of creating new welding consumables for joining high-strength low-alloy steels (HSLA) for ship construction [8].

There are many "rules of thumb" in physical metallurgy. For example as the strength of the steel is increased, the ductility (both elongation and reduction-in-area) as well as the fracture toughness (as measured by either the Charpy or dynamic tear test) often decrease. Of course, this is not always the case and explains why direct relationships between strength and ductility or toughness are rare. It is for this reason that we decided to utilize the neural network method to determine if better predictions of the ductility and fracture toughness could be made if either the yield or ultimate strength was included as an input variable along with the chemical composition and the cooling rate.

Data Base

The set of experimental data is summarised in Table 1 [1,2]. The independent variables are the chemical composition of the as-deposited weld metal, the cooling rate at 538˚C, the measured yield or ultimate strength. The dependent variables are the elongation, reduction-in-area, the measured Charpy V-notch values at –18 or –51˚C, or the dynamic tear test values at –1 or –29˚C. The cooling rate was determined from the welding parameters (voltage, current, welding speed), preheat, and thickness of the plate [9,10]. Table 1 gives the minimum, maximum, mean, and standard deviation each of the variables.

The dynamic tear test results are generated on welds which did not contain titanium. A detailed description of both the data set and the neural network employed is found in the prior study [1,2].

One aspect of avoiding over fitting in the development of a neural network requires that the data set be divided into a training and a test set. There are also other features described in [3-7] that implement automatic relevance determination. The model is at first produced using only the training data set. It is then used to see how it generalises on the unseen test data. By monitoring both the training and test errors, it is possible to select the single best model.

It is, however, possible that a committee of models can make a more reliable prediction than an individual model [6-7]. To do this, the best models are ranked using the values of the test errors. Committees are then formed by combining the predictions of the best L models, where $L = 1, 2, \ldots\ldots$ The size of the committee is given by the value of L. A plot of the test error of the committee versus its size L gives a minimum which defines the optimum size of the committee.

Table 1: The input and output variables. The concentrations are in wt% except for oxygen and nitrogen which are in parts per million by weight. The cooling rate is expressed in °C/s.

Variable	Minimum	Maximum	Mean	Std. Dev.
C	0.001	0.06	0.0307	0.0098
Mn	1.05	3.44	1.4361	0.1915
Si	0.05	0.4	0.2618	0.0555
Cr	0	0.21	0.0664	0.0530
Ni	1.66	5.63	3.1324	0.7800
Mo	0	1.23	0.5048	0.1452
Cu	0	0.48	0.1018	0.0766
S	0.001	0.012	0.0034	0.0019
P	0.001	0.015	0.0041	0.0026
Al	0.001	0.082	0.0066	0.0060
Ti	0.0008	0.3	0.0089	0.0181
Nb	0	0.069	0.0016	0.0041
V	0	0.031	0.0032	0.0042
B	0	0.01	0.0011	0.0021
O	109	627	216.7565	58.6969
N	6	135	29.8164	25.2642
Cooling rate, ˚C/s	1.32	76.17	27.1079	23.0104
YS, MPa	482	910	672.935	102.658
UTS, MPa	589	971	742.708	86.503
Elongation, %	3.5	29.2	20.8411	5.2370
Reduction-in-Area, %	7	84	94.6325	17.9575
CVN@-18˚C, J	8	358	181.9955	57.0641
CVN@-51˚C, J	3.8	242	143.6876	64.3903
DT@-1˚C, J	128	2606	1322.4916	538.1394
DT@-29˚C, J	80	2380	950.2694	583.3663

For each property, therefore, a committee of models was used to make predictions. Once the optimum committee is selected, it was retrained on the entire data set without changing the complexity of each model, with the exception of the inevitable, although relatively small, adjustments to the weights. Normally the error bars that are plotted represent the fitting error, the magnitude of which depends on the position in the input space. The additional error $□_{□}$ is not usually plotted, but it is constant and can be taken as the highest value of $□_{□}$ for any member of the committee of models, as listed in Table 2.

Table 2: The number of models in each committee, and the corresponding largest value of □□.

Property	Models	□□
UTS	6	0.061
YSUTS	14	0.047
EL	9	0.128
YSEL	8	0.127
UTSEL	18	0.130
RA	25	0.139
YSRA	4	0.117
UTSRA	19	0.140
CVN@-18˚C	1	0.055
YS CVN@-18˚C	80	0.109
UTS CVN@-18˚C	7	0.063
CVN@-51˚C	6	0.081
YS CVN@-51˚C	2	0.081
UTS CVN@-51˚C	11	0.080
DT@-1˚C	6	0.091
YS DT@-1˚C	2	0.098
UTS DT@-1˚C	10	0.233
DT@-29˚C	77	0.222
YSDT@-29˚C	3	0.136
UTSDT@-29˚C	6	0.139

Results and Discussion

Ultimate Strength

The ultimate tensile strength was predicted by adding the yield strength to the input variables. The data set consisted of 188 points. The results are shown in Fig, 1, where Fig.1a represents the predictions based on composition and cooling rate, and Fig. 1b is the predictions based on composition, cooling rate and yield strength. As might be expected, a better correlation is obtained when the yield strength is added as a dependent variable. It is useful to understand the significance of each input in influencing the UTS. The significance $\square_w$, which is plotted in Fig. 1c, is a measure to the extent to which an input variable can be correlated with variations in the output. In that sense it is rather similar to a partial correlation coefficient in linear regression analysis. It is therefore worth emphasizing that whereas $\square_w$ gives an indication of the correlation, it does not imply how sensitive the output is to the input – that information is in the weights. It is evident from Fig. 1c that the yield strength is an important parameter determining the UTS.

Elongation

There are three cases to consider: Fig. 2a is based on composition and cooling rate only; Fig. 2b is based on composition, cooling rate, and yield strength; Fig. 2c is based on composition, cooling rate, and ultimate strength. The number of data is 188 in all cases and the number of models in the committee is 9 in Fig 2a, and 8 for Fig. 2b and 18 for Fig. 2c.

The addition of the yield strength improves the predictability of the elongation (Fig. 2b), consistent with the observation in Fig. 2d that the yield strength is recognised to be a significant variable. On the other hand, the addition of the ultimate strength degrades the predictions. A possible reason why the inclusion of UTS does not help improve the estimation of elongation is that much of the elongation consists of uniform strain, whereas the ultimate tensile strength manifests at a point where necking begins. This is also seen in Fig. 2e, where the model perceived significance ($\square_w$) of the UTS is seen to be negligible.

Reduction-in-Area

The reduction of area has also been modelled in three ways: Fig. 3a is based on composition and cooling rate only; Fig. 3b is based on composition, cooling rate, and yield strength; Fig. 3c is based on composition, cooling rate, and ultimate strength. The number of data is 160 in all cases and the number of models in the committee is 25 in Fig 3a, and 4 for Fig. 3b and 19 for Fig. 3c. The addition of the yield or ultimate strength does not improve the predictability of the reduction of area. This is also reflected in the larger values of $\square_{\square}$ listed in Table 2.

An examination of the significance, σ_w (Figs. 3d,e), shows that consistent with these observations, the oxide forming elements, aluminum and oxygen, are important in determining the reduction of area.

Charpy V-Notch Tests

CVN@-18˚C

Fig. 4 depicts the predictions of the neural network for the case of the Charpy V-Notch tests at –18˚C. Fig. 4a is the original result, whereas Fig. 4b includes the yield strength as input, and Fig. 4c includes the ultimate strength. The original predictions are based on a data set of 602 points and a committee of 1 model. The addition of the yield strength resulted in a data set of 566 points and a committee of 80 models and the addition of the ultimate strength resulted in a data set of 568 points and a committee of 7 models.

CVN@-51˚C

Fig. 5 demonstrates the predictions of the neural network for the case of the Charpy V-Notch tests at –51˚C. Fig. 5a, which shows the original results, was determined using a committee of 6 models based on 602 points. Fig, 5b, with the yield strength as input, has a data set of 584 points and a committee of 2 models. Fig. 5c, ultimate strength as input, is based on a data set of 584 points and a committee of 11 models yielded the least correlation.

Dynamic Tear Tests

DT@-1˚C

Fig. 6a discloses the predictions of the neural network for the case of the dynamic tear test at –1˚C for a data set of 180 points and a committee of 6 models. The addition of the yield strength as a variable results in a data set of 180 points and a committee of 2 models. Substituting the ultimate strength for the yield strength reduces the data set to 98 points and the committee of models becomes 10. The best correlation appears to be based on chemistry and cooling rate only.

DT@-29˚C

Fig 7 shows the predictions of the neural network for the dynamic tear tests at –29˚C. The data set for all three cases was 180 points. Fig. 7a, the original results, has a committee of 77 models. The addition of the yield strength increases the number of models in the committee to 3, whereas the addition of the ultimate strength increases the number of models in the committee to 6. The addition of either yield or ultimate strength does not improve the predictability of the dynamic tear tests at –29˚C.

Use of the Models in Predictions

The performance of the models can be used to make predictions regarding trends as a function of each of the inputs. This is relatively straight forward for the calculation of the strength, ductility, and impact resistance as a function of composition and cooling rate. The addition of strength as a dependent variable complicates the predictive capability since it requires first calculating either the yield or ultimate strength and then calculating the desired property with the additional strength variable.

Summary

It is found that in most cases, the complex mechanical properties of a weld metal are best represented in terms of the chemical composition and cooling rate alone.

The inclusion of the yield or ultimate strength as inputs failed to improve the predictability of the neural network models, and did not provide any new insight into trends as a function of the inputs. Furthermore, the models become more difficult to use since a knowledge of the strength is required before a calculation can be conducted.

Acknowledgements

Funding support from the Office of Naval Research (Arlington, VA USA), and from the Cambridge Commonwealth Trust, is gratefully acknowledged.

References

1. E. A. Metzbower, J. J. DeLoach, Jr., S. H. Lalam and H. K. D. H. Bhadeshia: *Science and Technology of Welding and Joining* 6 (2001) 116.
2. E. A. Metzbower, J. J. DeLoach, Jr., S. H. Lalam and H. K. D. H. Bhadeshia: *Science and Technology of Welding and Joining*, in press.

3. D. J. C. MacKay, *Neural Comput.,* 4 (1992) 415.

4. D. J. C. MacKay, *Neural Comput*., 4(1992) 448.

5. D. J. C. MacKay, *Neural Comput*., 4 (1992) 698.

6. D. J. C. MacKay, *Mathematical Modeling of the Weld Phenomena III*, eds H. Cerjak and H. K. D. H. Bhadeshia, The Institute of Materials, London, (1997) 359-389.

7. H. K. D. H. Bhadeshia, *ISIJ International*., 39 (1999) 966-979.

Figure Captions

Fig. 1 Comparison of predicted and measured values of UTS for as deposited weld metal. The error bars represent +- 1□ values, where □ is standard deviation. (a) Predictions in which the yield strength is not included in the inputs. (b) Predictions in which the yield strength is included in the inputs. (c) The significance of each variable, for the model used in the calculations for Fig. 1b.

Fig. 2 Comparison between predicted and measured values of elongation for as deposited weld metals. (a) Calculations in which the strength is not included as an input variable. (b) Calculations in which the yield strength is one of the inputs. (c) Calculations in which the UTS is one of the inputs. (d) The significance of each variable for the model illustrated in 2b. (e) The significance of each variable for the model illustrated in 2c.

Fig. 3 (a-c) Comparison of predicted and measured reduction-in-area for as deposited weld metals. (d) The model perceived significance of each variable for the case where the yield strength is included as a variable. (e)

The model perceived significance of each variable for the case where the ultimate tensile strength is included as a variable.

Fig. 4 Comparison of predicted and measured Charpy V-notch energy at –18°C for as deposited weld metals

Fig. 5 Comparison of predicted and measured Charpy V-notch energy at –51°C for as deposited weld metals.

Fig. 6 Comparison of predicted and measured dynamic tear energy at –1°C for as deposited weld metals

Fig. 7 Comparison of predicted and measured dynamic tear energy at –29°C for as deposited weld metals

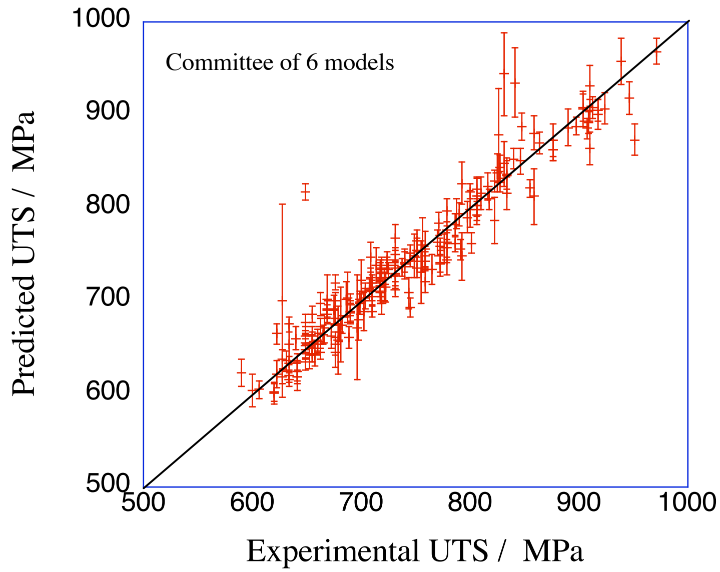

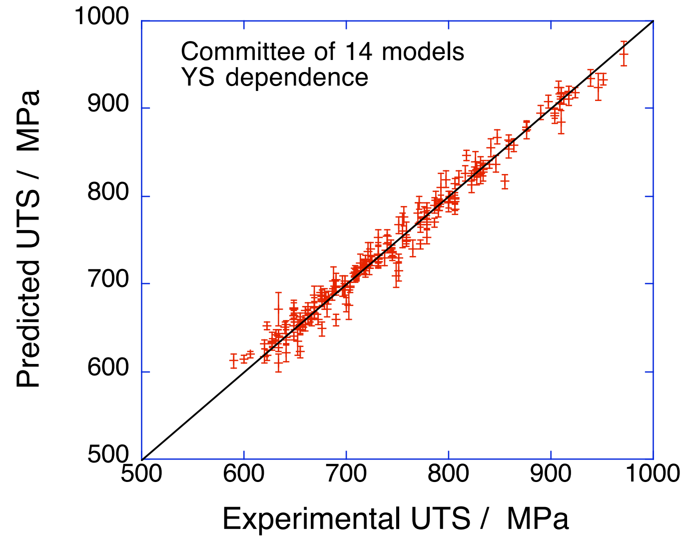

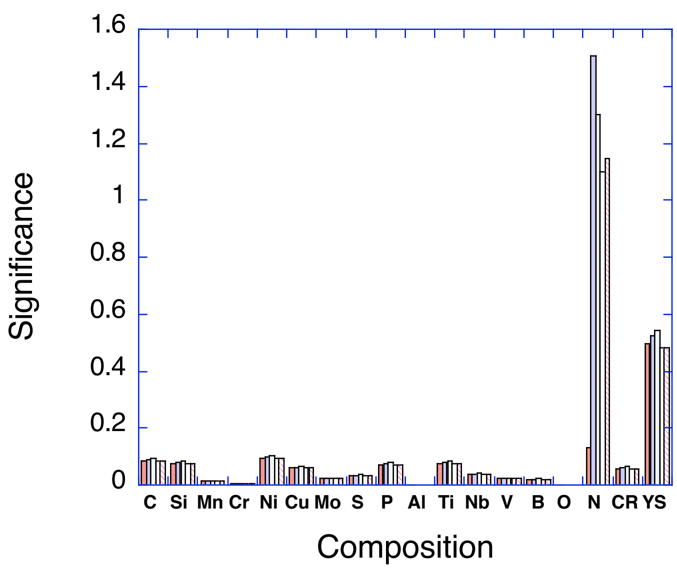

Fig. 1a, 1b, and 1c

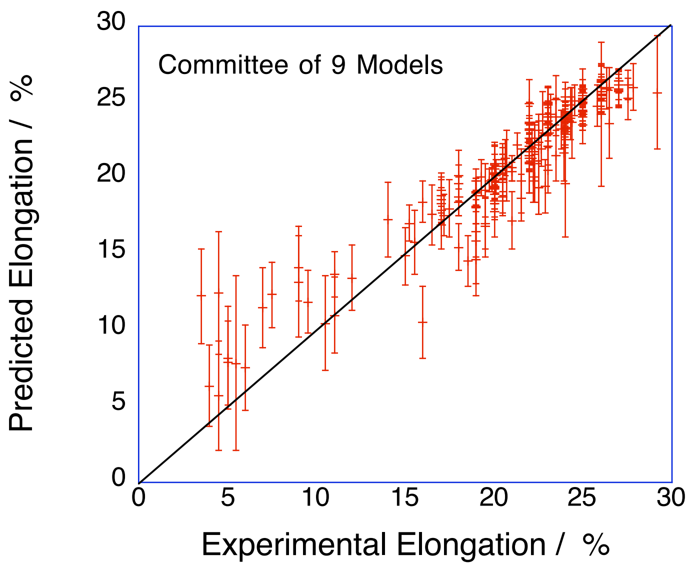

Fig. 2a, 2b, and 2d

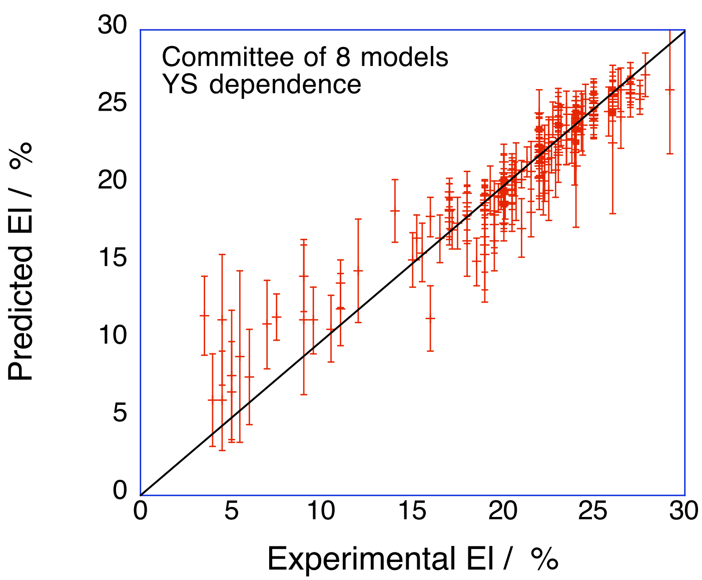

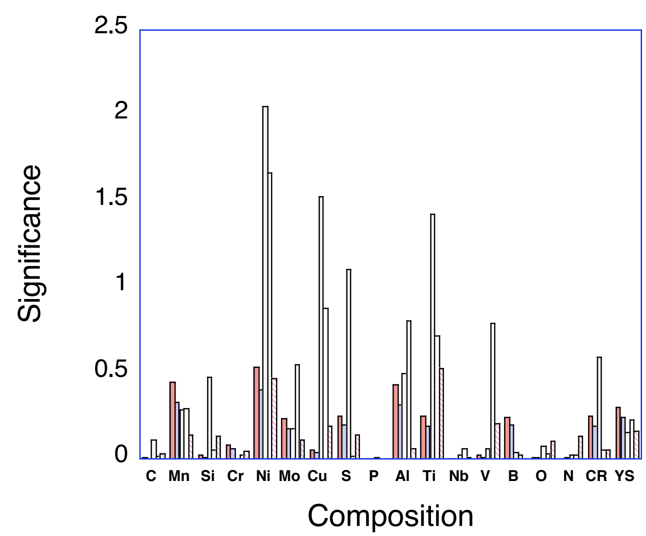

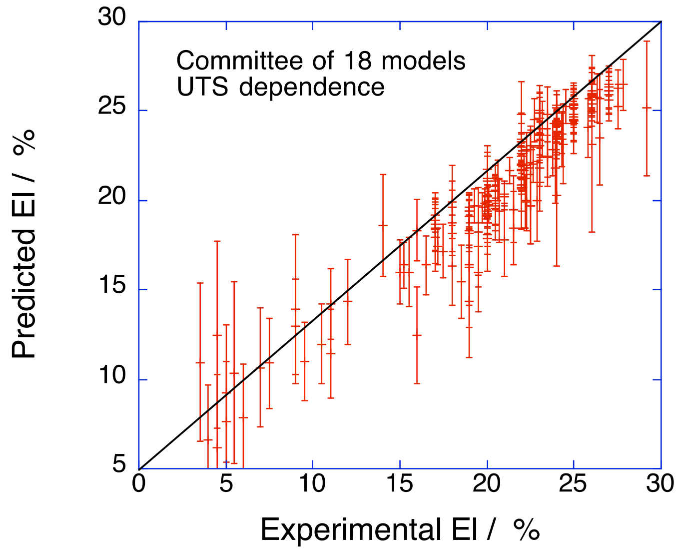
Committee of 18 models
UTS dependence
Predicted El / %
Experimental El / %
0
5
10
15
20
25
30

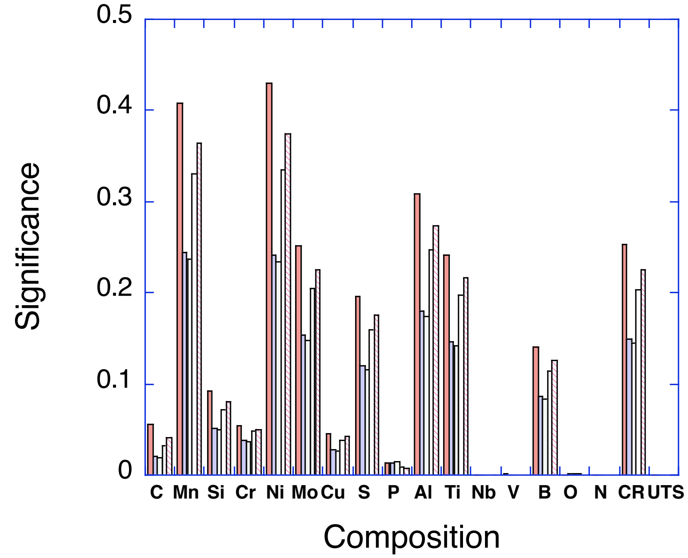
Significance
Composition
0
0.1
0.2
0.3
0.4
0.5
C
Mn
Si
Cr
Ni
Mo
Cu
S
P
Al
Ti
Nb
V
B
O
N
CR
UTS

Fig. 2c and 2e

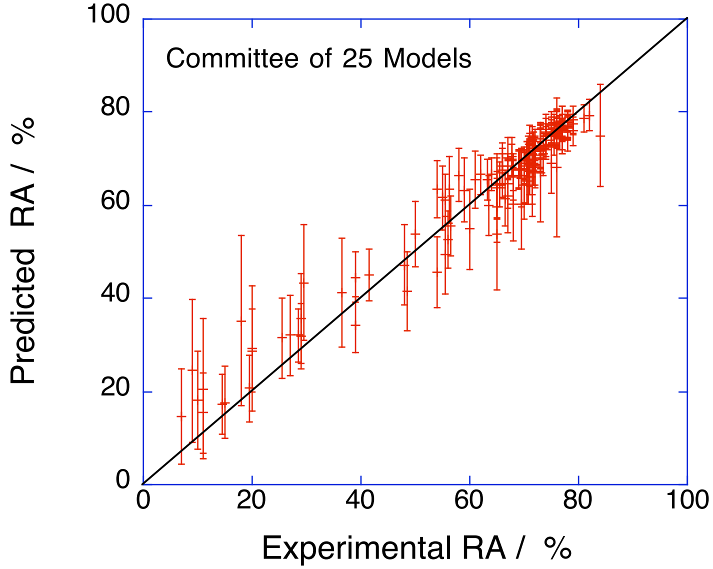

Fig. 3a, 3b, and 3d

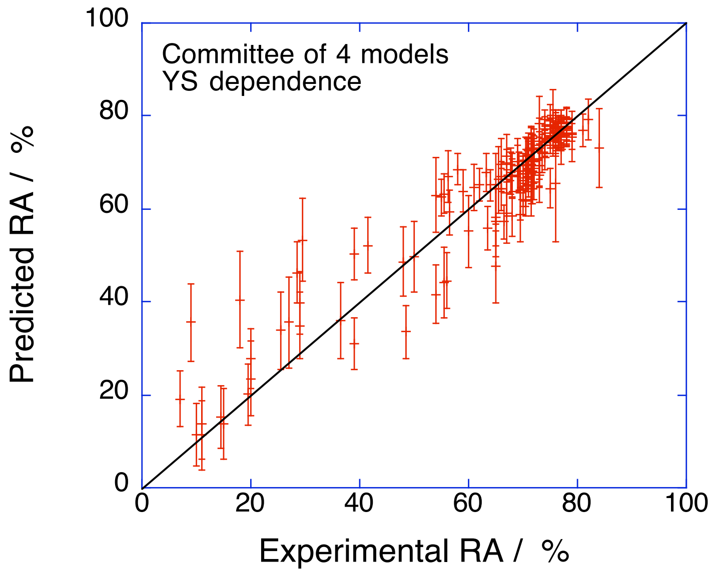

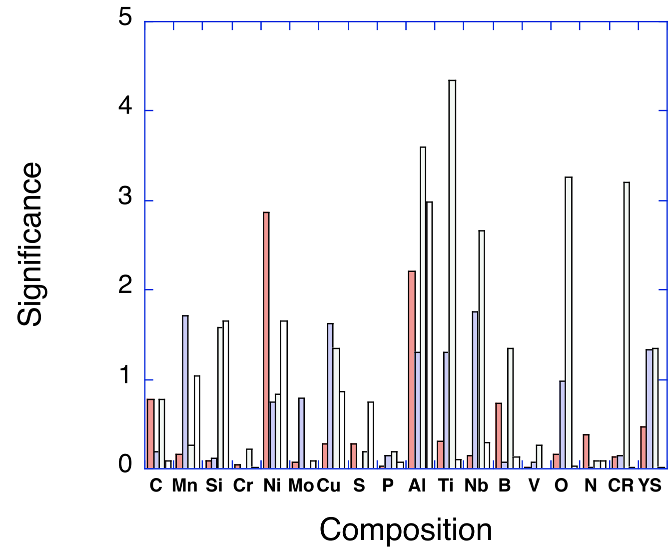

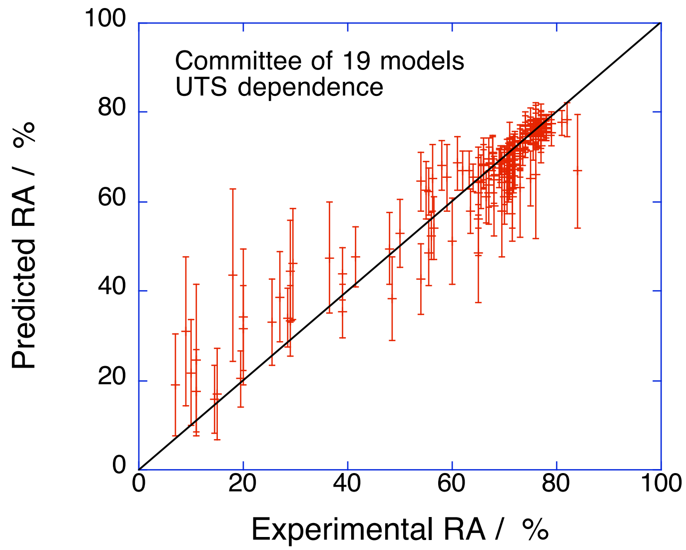

Committee of 19 models
UTS dependence
Predicted RA / %
Experimental RA / %
0
20
40
60
80
100

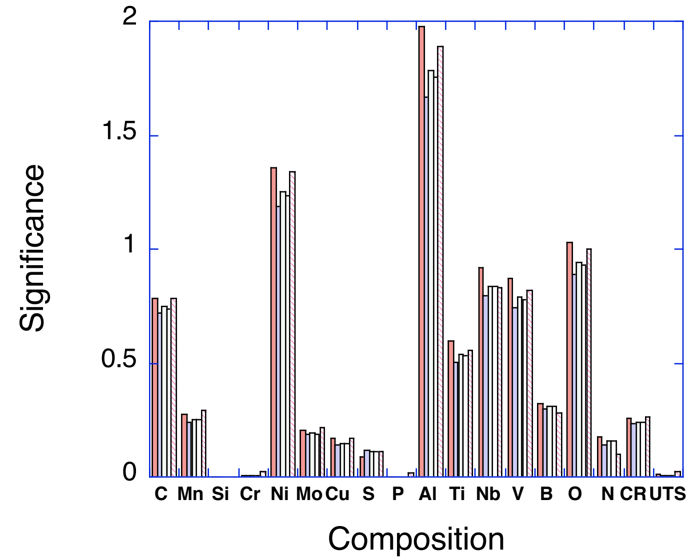

Significance
Composition
0
0.5
1
1.5
2
C Mn Si Cr Ni Mo Cu S P Al Ti Nb V B O N CR UTS

Fig. 3c and 3e

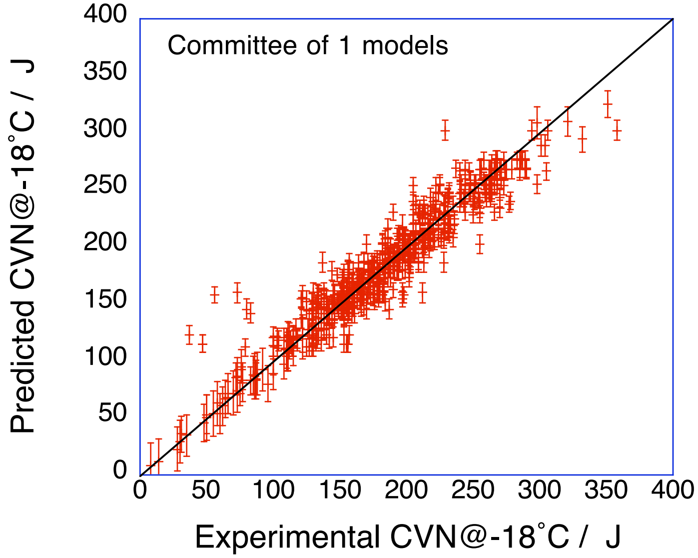

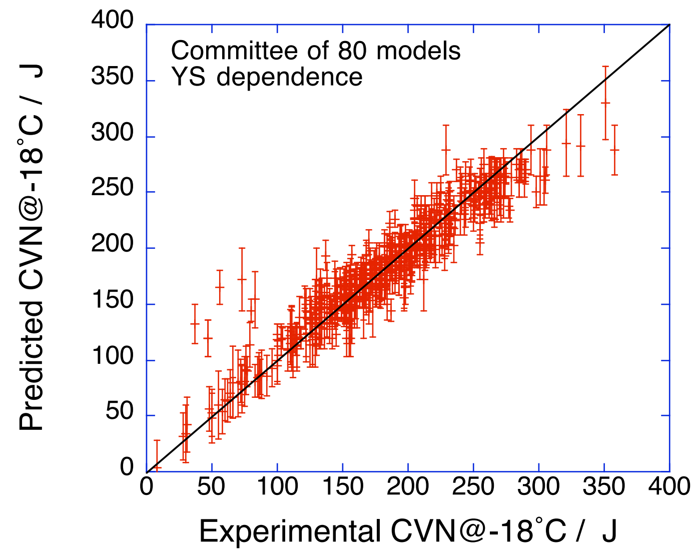

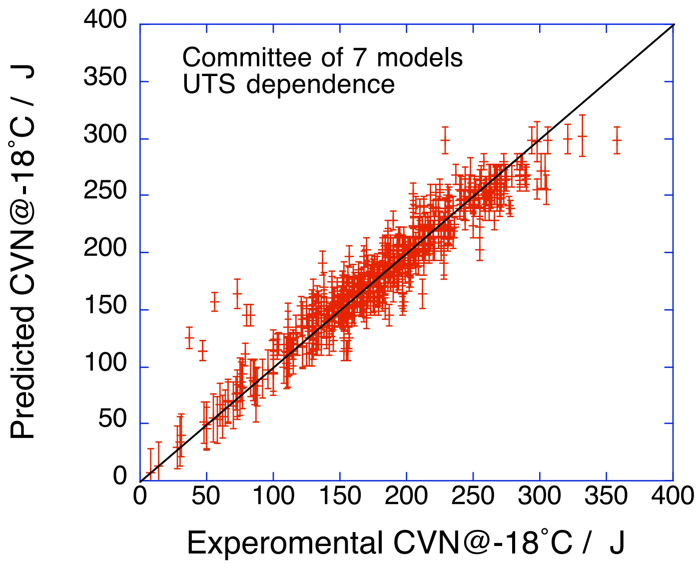

Fig. 4a, 4b, and 4c

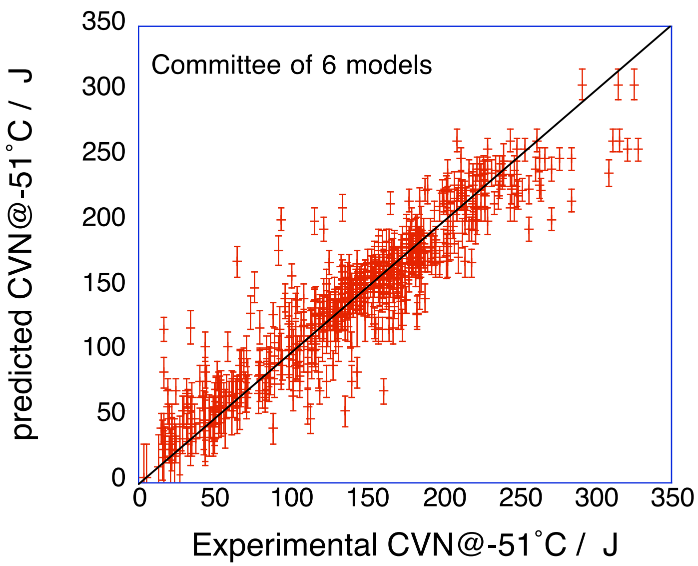

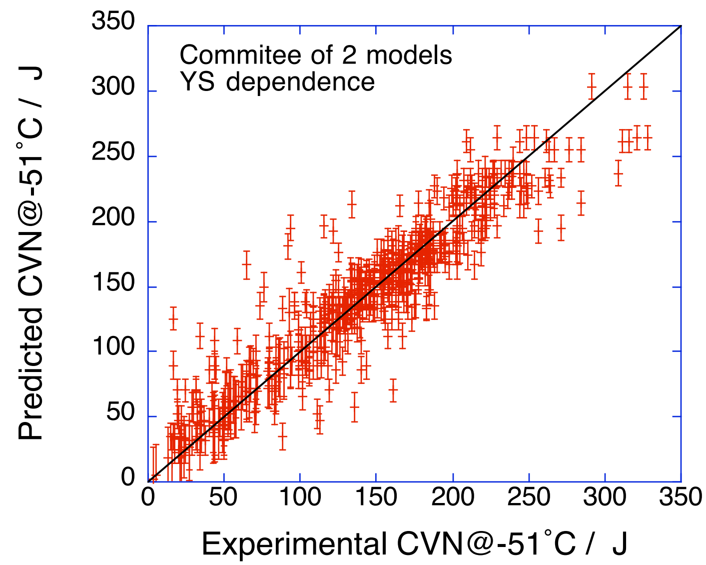

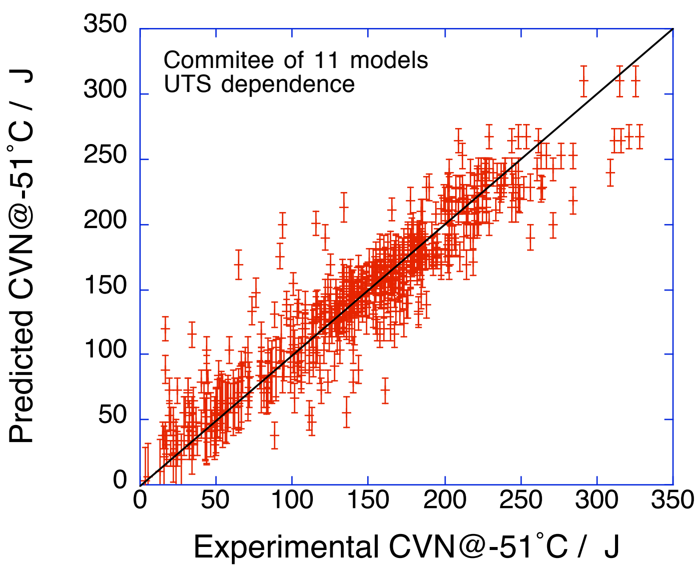

Fig. 5a, 5b, and 5c

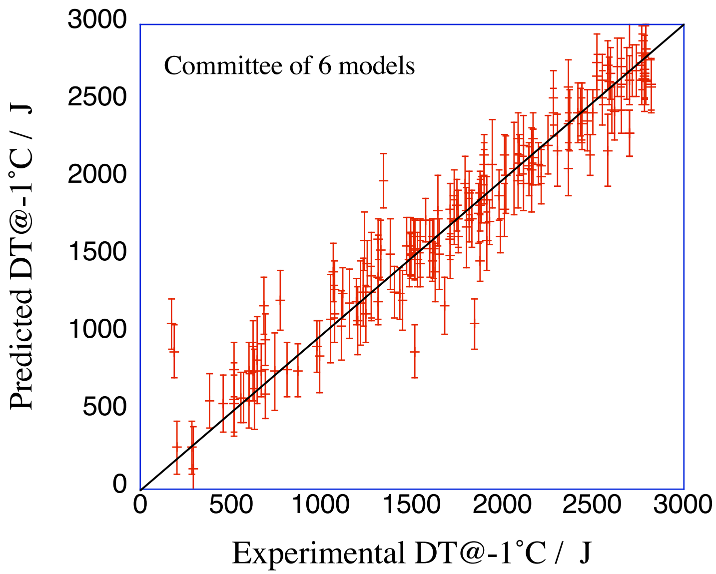

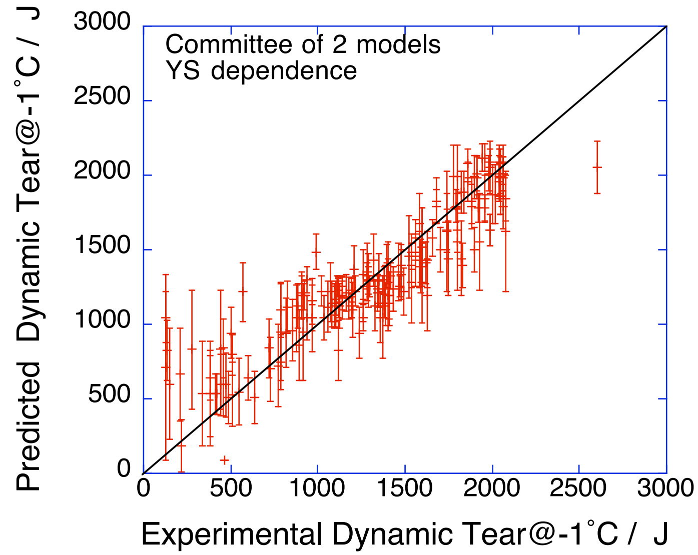

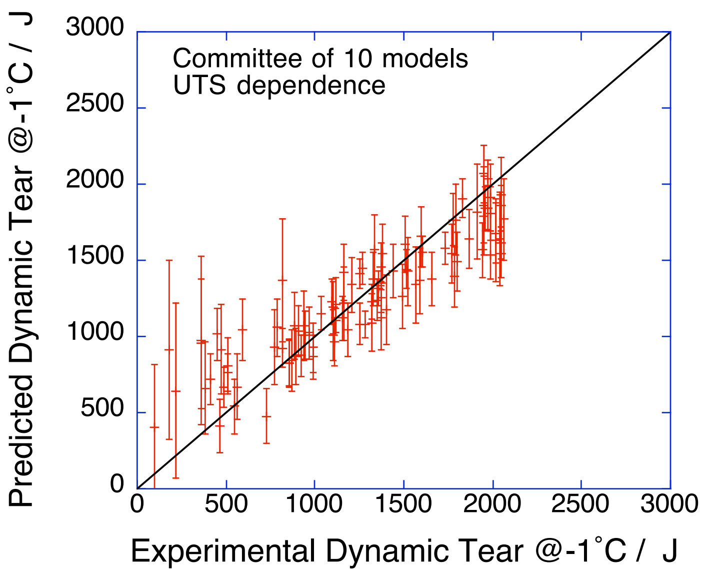

Fig. 6a, 6b, and 6c

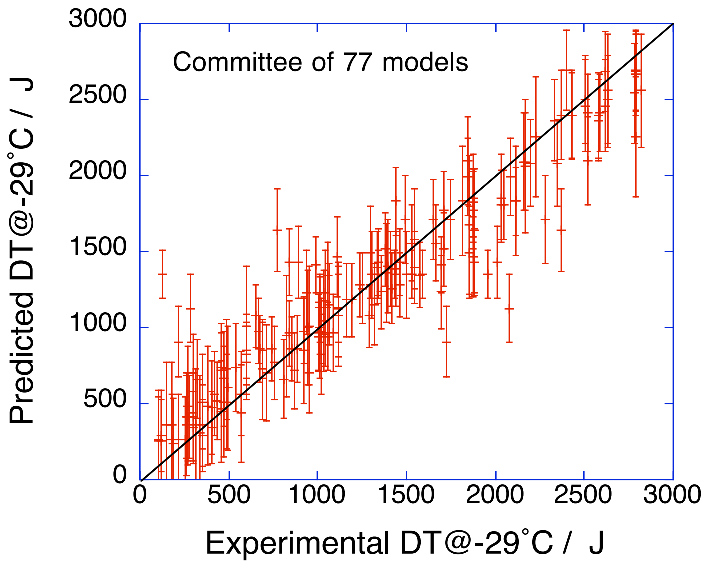

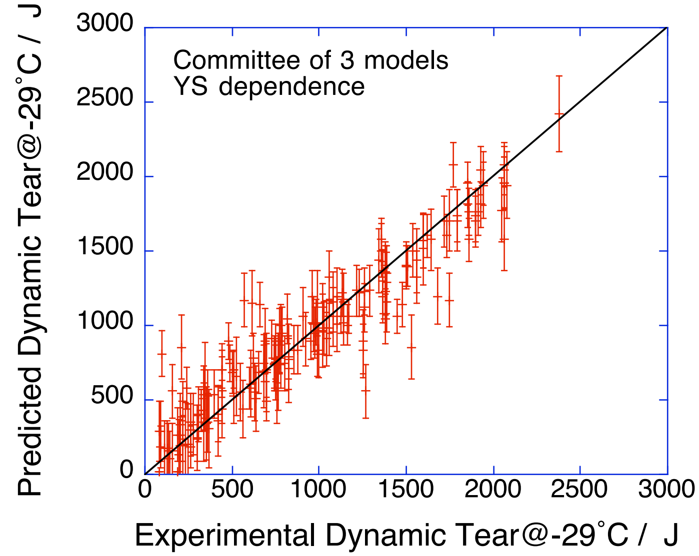

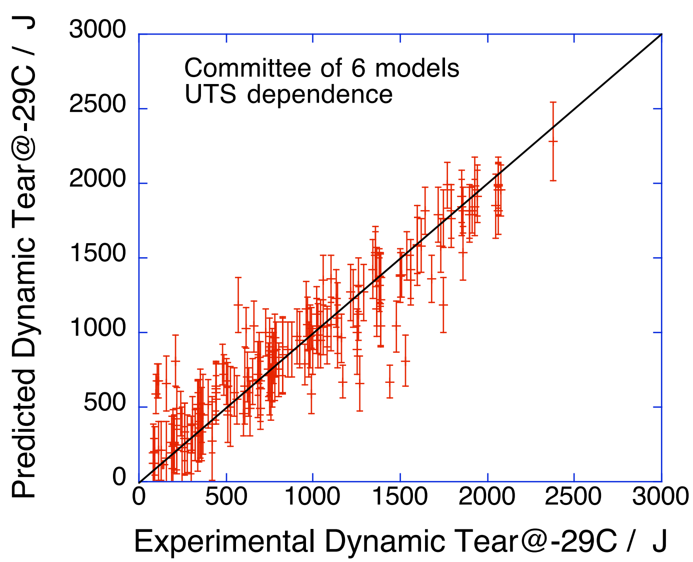

Fig. 7a, 7b, and 7c